Stereochemical Requirements for Receptor Recognition of the μ-Opioid Peptide Endomorphin-1

M. Germana Paterlini,* Francesca Avitabile,* Beverly Gaul Ostrowski,† David M. Ferguson,* and Philip S. Portoghese*

*Department of Medicinal Chemistry and Supercomputer Institute and †Department of Biochemistry, Biophysics, and Molecular Biology, University of Minnesota, Minneapolis, Minnesota 55455 USA

ABSTRACT A series of diastereoisomers of endomorphin-1 (EM1, Tyr[1]-Pro[2]-Trp[3]-Phe[4]-NH_2) have been synthesized and their potency measured using the guinea pig ileum assay. [D-Phe[4]]EM1 possessed 1/10 the potency of EM1, while potencies of [D-Tyr[1]]EM1 and [D-Trp[3]]EM1 were 50- and 100-fold lower, respectively. Drastic loss of activity occurred in the [D-Pro[2]]EM1 peptide. The structural determinants for the inactivity and reduced potency of the diastereoisomers were investigated using NMR spectroscopy and conformational analysis. Simulations of *trans*-[D-Pro[2]]EM1 using NOE-derived distance constraints afforded well-defined structures in which Tyr and Trp side chains stack against the proline ring. The inactivity of [D-Pro[2]]EM1 was explained by structural comparison with EM1 (Podlogar et al.,1998, *FEBS Lett.* 439:13–20). The two peptides showed an opposite orientation of the Trp[3] residue with respect to Tyr[1], thus suggesting a role of Pro[2] as a stereochemical spacer in orienting Trp[3] and Phe[4] toward regions suitable for μ-receptor interaction. The agonist activity of [D-Tyr[1]]EM1 and [D-Trp[3]]EM1 was attributed to their ability to adopt low-energy conformations that mimic those of EM1. The requirements for μ-receptor activation were examined further by comparing EM1 with the μ-peptide [D-Ala[2], MePhe[4], Gly-ol]-enkephalin (DAMGO). Conformations of DAMGO with a Tyr[1]-MePhe[4] phenyl ring separation of ~12 Å were found to mimic Tyr[1]-Phe[4] of EM1, thus suggesting overlapping binding modes between these two peptides.

INTRODUCTION

Morphine and endogenous opioid peptides share a common opioid core in which the spatial disposition of a cationic amine, a phenolic ring, and an additional hydrophobic group are necessary to elicit function at opioid receptors (Casy, 1993). However, the conformational flexibility of opioid peptides has hampered numerous attempts at determining the relationship between the solution conformation and activity using spectroscopic and modeling methods. Insights into the conformational requirements of peptide binding have been obtained through the synthesis of analogs with a more rigid backbone scaffold (Mosberg et al., 1983; Schiller et al., 1992), or by studies in media that promote structure, such as viscous solvents (Picone et al., 1990; Amodeo et al., 1998), lipids (Milon et al., 1990), or lyotropic liquid crystals (Kimura et al., 1997).

Two novel opioid peptides have recently been isolated from mammalian brains (Zadina et al., 1997). These tetrapeptides, Tyr-Pro-Trp-Phe-NH_2 and Tyr-Pro-Phe-Phe-NH_2, have been called endomorphins (denoted EM1 and EM2, respectively, in Fig. 1) because they are the first reported brain peptides with high affinity and selectivity for the μ-opioid receptor (Zadina et al., 1997). The endomorphin structures are particularly amenable to conformational studies, as they contain a conformationally restricted proline at the second position. As such, the endomorphins are in the same class of peptides as morphiceptin (Chang et al., 1981), PL017 (Chang et al., 1983), and Tyr-W-MIF-1 (Zadina et al., 1997), shown in Fig. 1, in which a Pro at the second position confers high selectivity on the μ-opioid receptor. The affinity of these peptides greatly depends on the nature of the amino acid at the fourth position. For example, the affinity increases fivefold upon substitution of Gly in Tyr-W-MIF-1 with a hydrophobic residue and more than 50 times if Phe replaces Gly, as in EM1 (Zadina et al., 1997). Similarly, Tyr-W-MIF-1 showed minimal activation of G-proteins, while the efficacy of EM1 is 65–78% that of the potent μ-opioid peptide [D-Ala[2], MePhe[4], Gly-ol]-enkephalin (DAMGO, Fig. 1) (Alt et al., 1998; Harrison et al., 1998; Narita et al., 1998; Sim et al., 1998).

The solution structure of EM1 has been reported using NMR spectroscopy and conformational analysis (Podlogar et al., 1998). The existence of a μ-selectivity pocket was proposed based on structural similarity with the μ-peptide PL017 structure. However, the structure of a single compound does not allow exploration of the full range of accessible pharmacophoric conformations. In this work, we have systematically inverted the stereochemistry at each of the four positions of EM1 to explore how changes in conformation affect the biological potency of EM1. By comparing diastereoisomers of different potency and activity at the μ-opioid receptor, it was possible to reduce the range of accessible conformers to a smaller number of "bioactive" candidates. The results have revealed the probable role of proline as a stereochemical spacer in receptor recognition and have allowed isolation of the role of each of the three aromatic residues in the activation of μ-opioid receptors by EM1. The putative bioactive conformation of EM1 was compared with that of DAMGO to evaluate any similarities or differences in the conformations of these two peptides.

Received for publication 6 July 1999 and in final form 2 November 1999.

Address reprint requests to Dr. M. Germana Paterlini, 308 Harvard Street SE, WDH, Minneapolis, MN 55455. Tel.: 612-626-3551; Fax: 612-626-4429; E-mail: germana1@vwl.medc.umn.edu.

0006-3495/00/02/590/10 $2.00

MATERIALS AND METHODS

Synthesis of endomorphin-1 analogs

EM1, [D-Tyr[1]]EM1, [D-Pro[2]]EM1, [D-Trp[3]]EM1, and [D-Phe[4]]EM1 were obtained from the Microchemical Facility of the University of Minnesota. The peptides were synthesized by a stepwise solid-phase procedure using

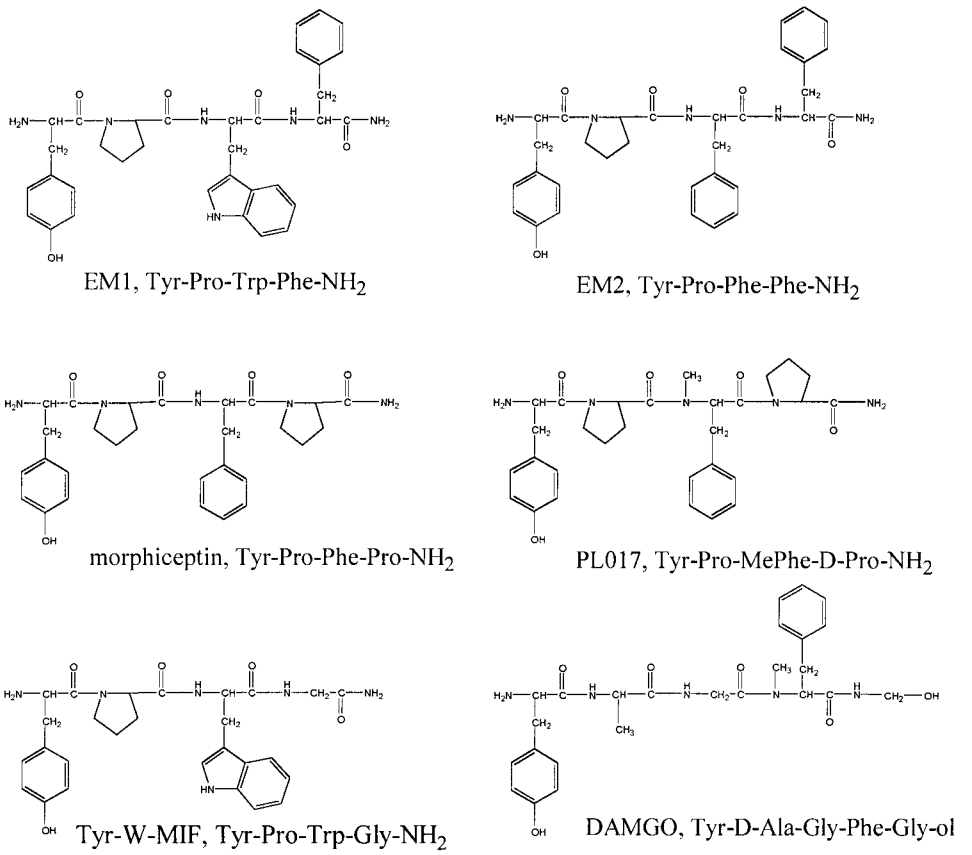

FIGURE 1 Schematic diagram of μ-selective opioid peptides discussed in the current study.

standard fluoren-9-ylmethoxy carbonyl (Fmoc) chemistry. The structure of the peptides was confirmed by amino acid analysis and fast-bombardment mass spectroscopy (FAB-MS). Purification was obtained using a high-performance liquid chromatography system with a reverse-phase C_{18} column. The purity was 88% for [D-Tyr^1]EM1 and 93% or greater for the remaining peptides.

Pharmacology: guinea pig ileal longitudinal method

The guinea pig ileal (GPI) preparation was prepared by the method of Rang (1964), and agonist activity was measured as described previously (Portoghese and Takemori, 1985; Schwartz et al., 1997). GPI preparations contain functional μ- and κ-opioid receptors. Evaluation of a possible antagonist component of [D-Pro^2]EM1 was accomplished by incubating the peptide (1 μM) for 15 min with the preparation before the testing with the μ-agonist morphine or the κ-agonist ethylketazocine. Pretreatment with antagonists nor-binaltorphimine (nor-BNI) (20 nM) (Portoghese et al., 1987) or naltrexone (100 nM) was employed to demonstrate interaction at κ- or μ-opioid receptors, respectively.

NMR spectroscopy

Five-millimeter tubes (Kontes, Vineland, NJ) and dimethyl sulfoxide-d_6 (DMSO-d_6) (99.9% isotopic purity; Cambridge Isotope Laboratories, Andover, MA) were used for NMR spectra acquisition. The peptide concentration was 8 mM in DMSO-d_6. A Varian INOVA 800-MHz and a Unity-INOVA 600 MHz Varian spectrometer with VNMR 6.1 software were used for one-dimensional (1-D) and two-dimensional (2-D) spectra, respectively. Proton 1-D spectra were acquired using 128 increments with 16K data size. A set of 1-D experiments with temperatures between 25°C and 45°C were performed to measure temperature coefficients of the amide protons. Two-dimensional spectra were acquired using standard pulse programs available in the Varian software library. TOCSY spectra were recorded at 25° and 45°C with mixing times of 50 and 60 ms, respectively, while mixing times of 400 ms and 300 ms were used for NOESY and DQF-COSY experiments at 25°C, respectively. ^{1}H-^{13}C HMQC data were collected with a proton spectral width of 5000 Hz and an acquisition time of 0.21 and 16 scans/increment; the carbon spectral width was 20,000 Hz with 512 increments in the ^{13}C dimension. Chemical shifts for ^{13}C were referenced from the DMSO peak position. NOESY experiments were also performed for a sample at 10 mM in 90% H_2O/10% D_2O at pH 4.1. Data were collected at 25°C with a mixing time of 400 ms. Water suppression was accomplished using the Watergate suppression sequence.

Data were processed using the NMRPipe suite of programs (Delagio et al., 1995). NOE intensities were classified into three groups according to a calibration against the peak intensity of nondegenerous geminal protons. The three groups (strong, medium, and weak) were placed in categories

TABLE 1 The effect of endomorphin-1 and its analogs on the guinea pig ileum preparation

Peptide	IC_{50} (nM) (n)*	Agonist potency Ratio†
EM1	6.7 ± 2.0 (3)	10.9 ± 2.9
[D]-Tyr^1]EM1	303 ± 101 (3)	0.24 ± 0.09
[D-Pro^2]EM1	28% (6)‡	—
[D-Trp^3]EM1	553 ± 135 (4)	0.14 ± 0.05
[D-Phe^4]EM1	127 ± 13 (3)	0.99 ± 0.64

*Values in parentheses are the number of determinations.
†The IC_{50} of the agonist divided by the IC_{50} of morphine in the same preparation.
‡Maximum response at 1 μM peptide.

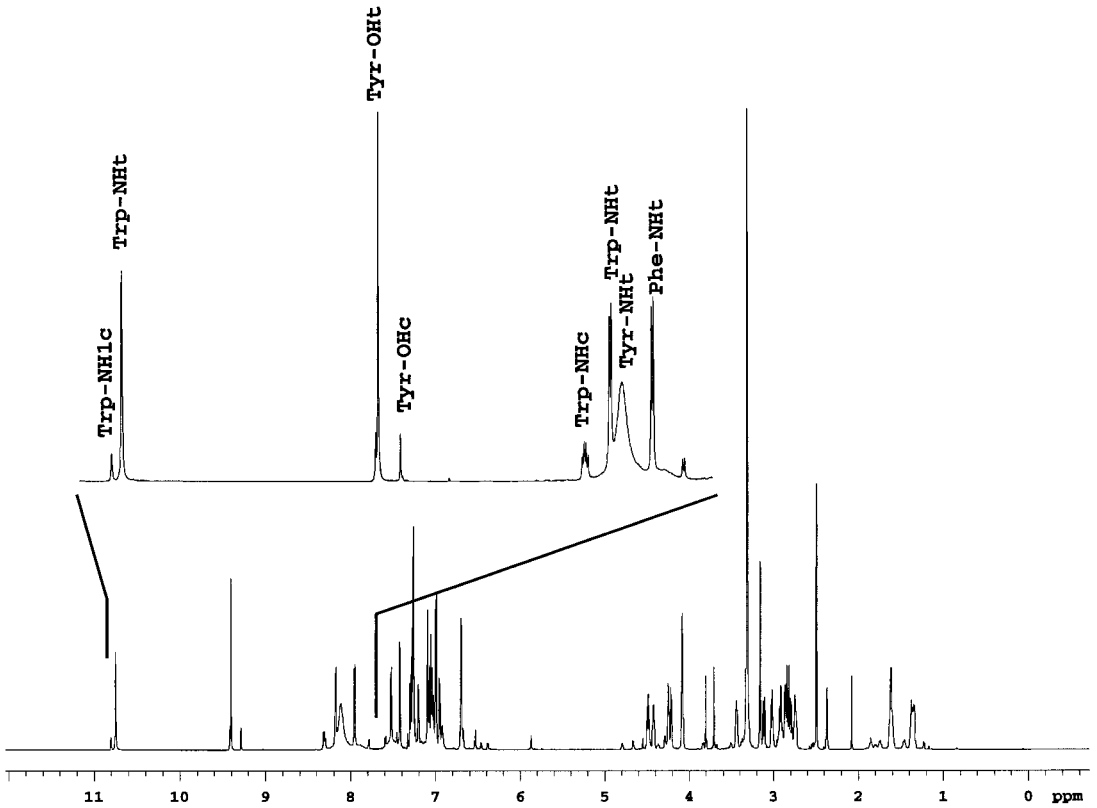

FIGURE 2 1-D 800-MHz NMR spectrum of [D-Pro^2]EM1 in DMSO-d_6 (8 mM, 25°C). Inset shows details of the amide, Tyr-OH, and Trp-NH_1 chemical shift region. The subscripts t and c refer to the *trans* and *cis* rotameters, respectively.

with upper distance limits of 2.5, 3.6, or 5.0 Å, respectively; all lower bounds were set at 1.8 Å (Williamson et al., 1985).

Conformational analysis

Systematic conformational searches were obtained using the SPASMS module of AMBER5.0 and the force field of Cornell et al. (1995) as recently updated for the peptide backbone parameters (parm96.dat) (Case et al., 1997). Energy minimization was carried out without a nonbonded cutoff to a convergence of 0.0005 in the gradient and a distance-dependent dielectric constant of 4*r*. The peptide was considered uncharged to minimize N- and C-termina artifacts. A simulated annealing protocol was used to obtain NMR-derived structures. A set of 200 randomly generated conformations was subjected to a 15-ps protocol during which the temperature of the system was increased to 1200 K and then rapidly cooled. The restraining potential was a flat square-bottom potential with parabolic sides and a force constant of 32 kcal/mol. The structures were then energy minimized and clustered using PADRE (Stahl and Walter, 1995), with a 0.85 Å cutoff for the rms deviation between structures.

Molecular dynamics simulations

Molecular dynamics simulations in aqueous solutions were obtained using AMBER5 (Case et al., 1997), by placing the peptides in a box with dimensions of 36 × 34 × 32 Å, containing a total of 1195 equilibrated water molecules. After 500 steps of energy minimization, the system was equilibrated by raising the temperature from 0 to 100 K for 5 ps, from 100 to 300 K for 15 ps, and continuing at 300K up to 100 ps under constant volume conditions. NOE-derived distance constraints were imposed during the first 10 ps of simulation and then slowly released up to 50 ps, after which they were set to zero. Simulations were then continued at constant pressure at 300 K with no constraints up to the indicated time.

TABLE 2 Observed NOE cross-peaks of [D-Pro^2]EM1 in DMSO-d_6

NOE observed	NOE* intensity	NOE observed	NOE* intensity
W_1-W_{NH}	m	W_{NH}-F_{NH}	s
W_1-W_β	w	F_{NH}-F_β	m
W_1-P_β	m	F_{NH}-$F_{\beta'}$	s
W_1-$P_{\beta'}$	m	F_{NH}-$F_{3,5}$	w
W_1-P_δ	w	F_{NH}-P_α	m
W_4-P_β	w	F_{NH}-P_β	w
W_4-$P_{\beta'}$	w	F_{NH}-$P_{\beta'}$	w
W_2-F_{NH}	m	F_{NH}-W_α	s
W_2-P_β	s	F_{NH}-W_β	m
W_2-$P_{\beta'}$	m	F_{NH}-$W_{\beta'}$	s
W_{NH}-W_β	m	F_{NH}-W_4	w
W_{NH}-$W_{\beta'}$	s	$Y_{2,6}$-P_δ	m
W_{NH}-W_2	m	$Y_{2,6}$-$P_{\delta'}$	m
W_{NH}-W_4	w	$Y_{2,6}$-P_β	w
W_{NH}-P_α	s	$Y_{2,6}$-$P_{\beta'}$	w
W_{NH}-P_β	s	$Y_{3,5}$-$P_{\delta'}$	m
W_{NH}-$P_{\beta'}$	s	$Y_{3,5}$-P_γ	w
W_{NH}-P_δ	m	$Y_{3,5}$-$P_{\gamma'}$	w

*NOE intensities are classified as weak, w < 5.0 Å; medium, m < 3.6 Å; or strong, s < 2.9 Å.

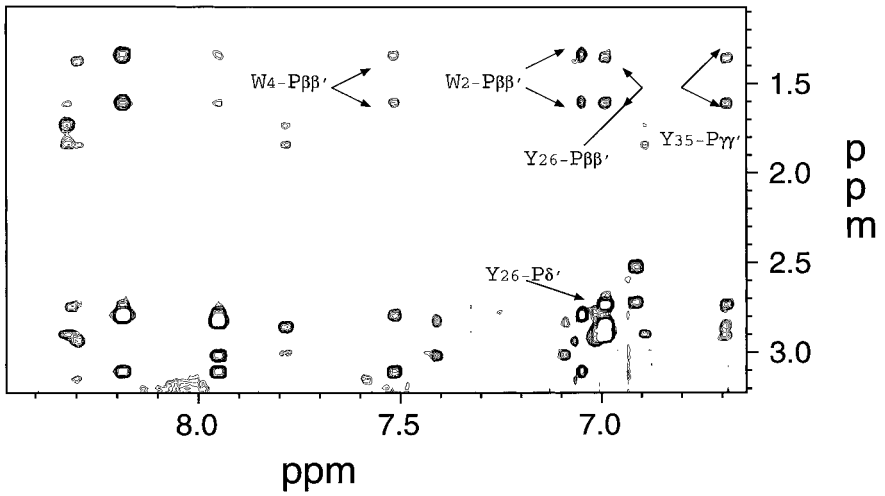

FIGURE 3 Part of the 600-MHz NOESY spectrum of [D-Pro^2]EM1 in DMSO-d_6 (8 mM, 25°C), showing correlation of proline ring protons with Trp and Tyr aromatic ring protons.

RESULTS

Endomorphin-1 and its diastereoisomers were evaluated for their biological activity, using the electrically stimulated GPI preparation (Portoghese and Takemori, 1985) (Table 1). Endomorphin-1 was 10-fold more potent than morphine and twofold more potent than DAMGO (results not shown), in agreement with a previous report (Zadina et al., 1997). Significantly, inversion of the Tyr^1 chiral center afforded a 50-fold reduction in potency relative to EM1. Inversion of Phe^4 resulted in a 10-fold loss of potency, while that of [D-Trp^3]EM1 was 100-fold lower. Activity was lost upon inversion of chirality at Pro^2 in the [D-Pro^2]EM1. This was due to the inability of this peptide to fully activate opioid receptors at a concentration (1 μM) that was $\geq$100-fold greater than the IC_{50} value of EM1. Furthermore, [D-Pro^2]EM1 was not an antagonist at either the μ- or κ-receptor, as it was unable to shift the dose-response curve of either morphine or ethylketazocine. While EM1 has a 20,000-fold selectivity over the κ-receptor (Zadina et al., 1997), it was unlikely that the diastereoisomers could show agonist activity at the κ-receptor. This was indeed the case, given that incubation of the GPI with the κ-selective antagonist norBNI did not shift the dose-response curves of the diastereoisomers. The interaction with opioid receptors was demonstrated by the nanomolar potency of naltrexone in antagonizing the agonism of the peptides.

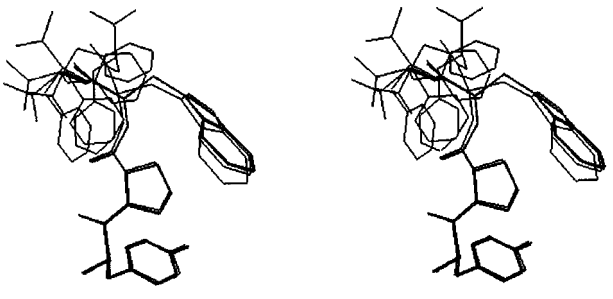

FIGURE 4 Low-energy conformations of [D-Pro^2] EM1consistent with NOE data. Structures are overlapped by rms fit of the backbone atoms of Pro, Trp, and Phe.

The 1-D NMR spectrum of [D-Pro^2]EM1 in DMSO-d_6 (Fig. 2) exhibited two populations of conformers corresponding to the *cis* and *trans* isomers. Interestingly, the relative chemical shifts between the major and minor conformers of the Tyr-OH and Trp-NH_1 protons were in an opposite relation compared to those observed in EM1 in DMSO-d_6 (Podlogar et al., 1998). The assignment of the spectral features to either *cis* or *trans* isomer was therefore confirmed using HMQC spectra. The difference between the ^{13}C chemical shifts of β (27.94 ppm) and γ (23.02 ppm) carbons of [D-Pro^2] EM1 was less than 5 ppm, which is typical of the *trans* conformation of proline (Dorman and Bovey, 1973; D'Ursi et al., 1992). The major isomer was therefore assigned to the *trans* conformation. Integration of the two peaks at 10.75 and 10.80 ppm gave 11% *cis* and 89% *trans* populations. Spectral features corresponding to the *cis* isomer presented additional complexity, as three separate forms of this isomer could be distinguished in both the 1-D and TOCSY data for DMSO-d_6.

The amide proton temperature coefficients, $\Delta\delta_{NH}$, of both *trans*- and *cis*-EM1were found to be in excess of 3.0×10^3 ppm/ K, indicating an absence of intramolecular hydrogen bonds in DMSO-d_6. The smaller $\Delta\delta_{NH}$ value of Trp ($\Delta\delta_{NH} = 3.5 \times 10^3$ ppm/ K) compared to Phe ($\Delta\delta_{NH}$(Phe) $= 5.5 \times 10^3$ ppm/ K) in the *trans* isomer suggests that this amide is less accessible to solvent. Changes in spectral bandwidth or C_α proton chemical shifts were not observed between 0.5 and 8 mM in DMSO-d_6, suggesting that aggregation does not occur at the concentration used here. This result is in agreement with the lower tendency of cationic opioid peptides to aggregate compared to dipolar peptides (Higashijma et al., 1978; Carpenter et al., 1996).

A total of 36 NOE cross-peaks were observed for the *trans* isomer in DMSO-d_6 (summarized in Table 2). Relevant regions of the NOE spectrum are shown Fig. 3. All but one of the NOE cross-peaks from backbone protons corresponded to sequential (i, $i + 1$) interactions with an addi-

TABLE 3 Minimum-energy conformations of Tyr-D-Pro-NMe, Tyr-Pro-NMe, and D-Tyr-Pro-NMe*

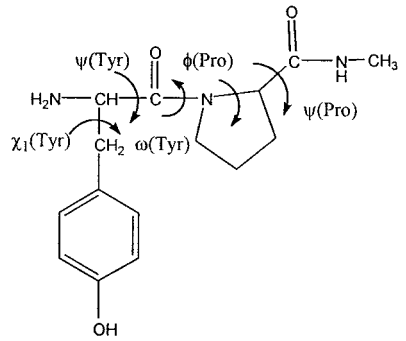

				Tyr			Pro	
Peptide	No.	$\Delta E^{\dagger}$	$v^{\ddagger}$	ψ	ω	χ_1	ϕ	ψ
Tyr-D-Pro-NMe	1D	0.00	0.65	136.3	177.8	−177.8	54.0	45.5
	2D	0.92	0.14	104.9	2.9	−173.5	67.3	49.4
	3D	1.31	0.07	127.4	3.1	−63.1	59.6	46.7
	4D	1.51	0.05	147.3	179.9	67.3	52.0	45.7
	5D	1.77	0.03	−68.0	−178.1	172.2	52.7	46.5
	6D	1.79	0.03	144.7	−178.8	−63.4	52.1	45.8
	7D	1.91	0.03	134.2	3.6	69.5	61.7	50.1
	8D	4.79	0.00	−74.3	8.8	173.6	58.0	48.6
	9D	4.84	0.00	−45.7	−177.6	71.5	53.5	49.9
	10D	4.91	0.00	−64.7	−177.1	−65.0	54.6	44.9
Tyr-Pro-NMe	1L	0.00	0.69	127.3	−177.2	178.5	−71.7	−51.1
	2L	0.67	0.22	137.8	−2.6	−176.3	−72.8	−38.2
	3L	1.53	0.05	149.8	−178.0	70.8	−69.9	−51.7
	4L	2.42	0.01	151.4	−3.1	68.0	−72.4	−38.6
	5L	2.45	0.01	150.1	−0.3	−65.2	−72.6	−39.8
	6L	2.66	0.01	149.0	179.1	−63.3	−69.8	−40.4
	7L	4.72	0.00	−59.4	−178.3	178.3	−69.8	−38.1
D-Tyr-Pro-NMe	1	0.00	0.63	−136.2	−178.6	177.6	−56.0	147.9
	2	0.7	0.21	−110.5	−2.4	173.9	−65.6	143.4
	3	1.4	0.06	−147.6	179.5	−67.3	−54.1	136.7
	4	1.8	0.03	−144.8	178.4	63.0	−54.2	136.9
	5	1.9	0.03	−121.9	−0.2	70.4	−60.4	153.7
	6	2.1	0.02	−134.3	−2.9	−69.3	−62.3	136.5
	7	2.8	0.01	66.9	175.2	−173.0	−55.5	133.0
	8	4.8	0.00	65.1	176.7	65.1	−56.2	139.1
	9	4.9	0.00	74.0	−7.5	−173.8	−58.9	144.0
	10	4.9	0.00	46.6	175.0	−69.0	−52.6	133.9

*Angles are defined in the schematic above. All angles are in degrees.
$^{\dagger}\Delta E = E - E°$, where $E°$ = 17.35 kcal/mol for Tyr-D-Pro-NMe, $E°$ = 15.96 kcal/mol for Tyr-Pro-NMe, and $E°$ = 16.1 kcal/mol for D-Tyr-Pro-NMe.
‡Statistical weights, expressed as a normalized Boltzmann factor $v_i = \exp(-\Delta E_i/RT)/\Sigma_i(-\Delta E_i/RT)$, where T = 300 K and R is the gas constant.

tional (*i, i* + 2) NOE signal between Pro-C_αH and Phe-NH. NOE cross-peaks were observed between the side chains of Pro and Trp and Pro and Tyr (Fig. 3), suggesting stacking of the two aromatic rings against proline. NOE data arising from the *cis* isomer of the peptide could not be fully assigned because of a low signal-to-noise ratio in addition to the spectral complexity of the *cis* isomer. Structural NOE cross-peaks were not observed for [D-Pro^2]EM1 in aqueous solution.

The NOE cross-peaks for the *trans* isomer were classified as weak (w), medium (m), and strong (s) and used as distance constraints in the simulated annealing protocol. Distances were assigned as s < 2.9 Å, m < 3.6 Å, and w < 5.0 Å, with a closest distance limit of 1.8 Å (Williamson et al., 1985). Of the 200 conformations generated in this fashion, five unique structures remained after clustering (shown in Fig. 4). No significant violations of NOE distance constraints were observed. A comparison among the five structures yielded a rms deviation of 0.84 ± 0.35 Å for the backbone atoms and an all-atom rms of 1.53 ± 0.43 Å. The deviations were largely due to Phe^4, which is less structurally defined because NOE cross-peaks between its aromatic ring and the other residues were not observed. Tyrosine and Trp side chains, however, were well characterized, with rotamers $\chi_1(\text{Tyr}) = t$ and $\chi_1(\text{Trp}) = g^-$.

The proline residue functions as a spacer between the tyramine moiety of Tyr and the aromatic residues at positions 3 and 4. Stereochemical inversion at Pro could affect either the conformation of the preceding (Tyr^1) or following

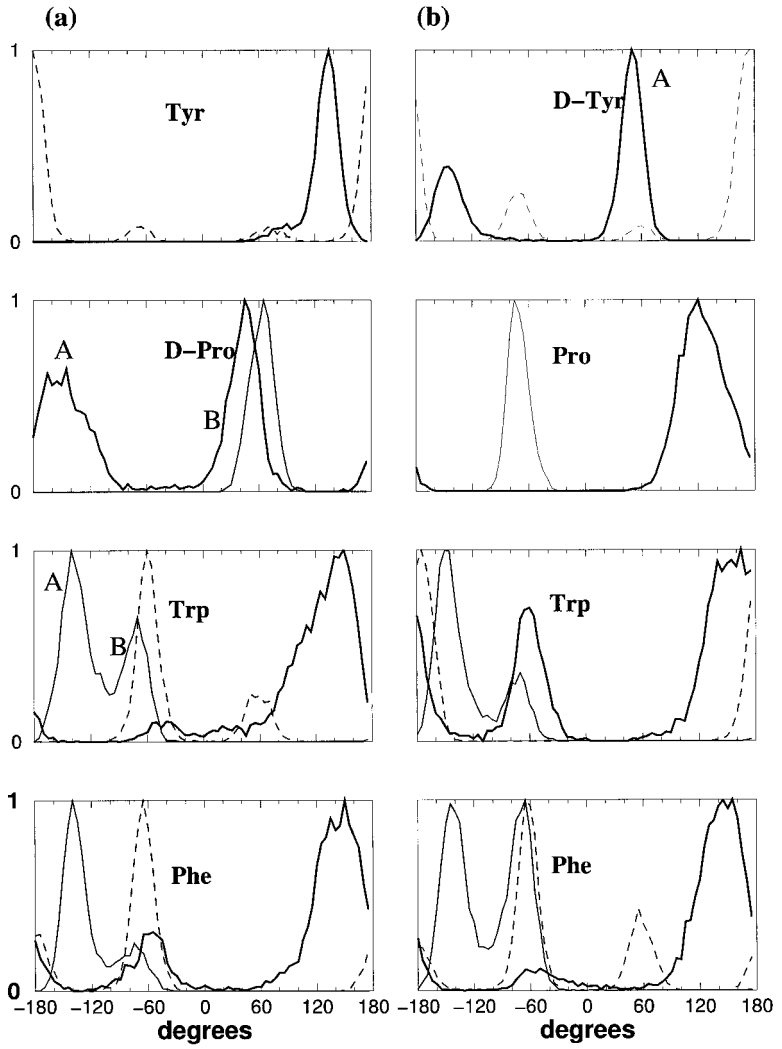

FIGURE 5 (*a*) Distribution of dihedral angles during a 4-ns simulation of solvated [D-Pro^2]EM1. Labels A and B denote the two major conformations observed during the trajectory. (*b*) Distribution of dihedral angles during a 6-ns simulation of solvated [D-Tyr^1]EM1. Angles shown: ϕ (*thin line*), ψ (*heavy line*), χ_1 (*dashed line*).

(Trp^3) residue, effectively changing the relative orientation of these two residues. The effect of chirality on the conformation of the Tyr-Pro fragment was examined using systematic conformational searches on the fragments Tyr-Pro-NMe, Tyr-D-Pro-NMe, and D-Tyr-Pro-NMe by varying the ψ(Tyr), ω(Tyr), and χ^1(Tyr) dihedral angles. Proline was placed in the α ($\phi = -70°$, $\psi = -50°$) or β ($\phi = -70°$, $\psi = 120°$) conformation, yielding similar results in the two cases.

The calculated *cis/trans* population ratios of 26/74% for Tyr-Pro-NMe and 23/77% for Tyr-D-Pro-NMe (Table 3) are in good agreement with the NMR data of EM1 (Podlogar et al., 1998) and its [D-Pro^2] diastereoisomer. The lowest energy conformer is similar in the two L-Tyr peptides and corresponds to a conformation with ψ(Tyr) in an extended or β conformation, *trans*-ω(Tyr), and *trans*-χ_1(Tyr) (conformations 1D and 1L in Table 3). Conformations with ψ(Tyr) $\approx 140°$ are preferred over those with ψ(Tyr) $\approx -65°$, in agreement with previous computational studies of Pro-containing peptides (Némethy et al., 1992). D-substitution of Tyr resulted in a reversal of the ψ(Tyr) dihedral angle, with conformations with ψ(Tyr) $\approx -135°$ preferred over those with ψ(Tyr) $\approx 65°$ (Table 3).

The conformational properties of [D-Pro^2]EM1 and [D-Tyr^1]EM1 were further examined using molecular dynamics simulations with explicit aqueous solvent. The distribution of backbone dihedral angles during a 4-ns simulation of [D-Pro^2]EM1 showed correlated motion in the Pro-Trp region, where two major conformations are sampled (conformations A and B in Fig. 5 *a*), while conformational sampling of Phe was independent of the other residues. Of the two conformations observed, A, with ψ(Pro) $= -150°$ and ϕ(Trp) $= -140°$, resulted in interactions between the Tyr, Pro, and Trp side chains and closely resembled the NMR-derived structure, with rms deviations of ~1–1.5 Å. The side-chain dihedral angles showed conformational preferences for χ_1(Tyr) $= t$, χ_1(Trp) $= g^-$, and χ_1(Phe) $= g^-$. Intramolecular hydrogen bonds were not observed throughout the simulation. Molecular dynamics simulations of the [D-Tyr^1]EM1 peptide (Fig. 5 *b*) showed trajectories of the Pro-Trp-Phe residues similar to those observed for EM1 (Podlogar et al., 1998). However, stereochemical inversion resulted in a reversal of the ψ(Tyr) dihedral angle, and, in this case, both the ψ(Tyr) $= 65°$ and ψ(Tyr) $= -135°$ conformations were populated.

The conformational dynamics of EM1 and its [D-Pro^2] and [D-Tyr^1] diastereoisomers were compared with those of DAMGO. This peptide exists in *cis-trans* equilibrium with respect to the Gly^3-MePhe^4 amide bond, but the most populated *trans* conformation was proposed to represent the bioactive form of the peptide based on NMR data and conformational analysis (Penkler et al., 1993). The *trans* isomer was therefore chosen for molecular dynamics simulations in explicit solvent. Calculations were performed on the N-terminal tetrapeptide-methylamide fragment, Tyr-D-Ala-Gly-MePhe-N′-CH_3 (*t*TAGP), to facilitate comparison with a previous conformational analysis (Penkler et al., 1993). Results are shown in Fig. 6. The first two residues sampled a wider range of conformations compared to the Tyr-Pro fragment (Figs. 5 and 6), as the angles ψ(Tyr) = −60° and ϕ(D-Ala) = 140° were also populated. The sharp distributions at ψ(MePhe) = 50° and χ_1(MePhe) = −60° reflected the steric restriction imparted by the *N*-methyl group of MePhe. The "hinge" region, comprising ψ(D-Ala) and ϕ(Gly), however, is flexible and has the effect of changing the relative orientation and distance, *D*, of the two aromatic groups. The great majority of structures had *D* values between 8 and 14 Å, but structures with $D \approx 6$ Å and $D \approx 17$ Å occurred as well. Overall, MD simulations resulted in a more exhaustive conformational sampling compared to previous approaches using conformational searches (Penkler et al., 1993).

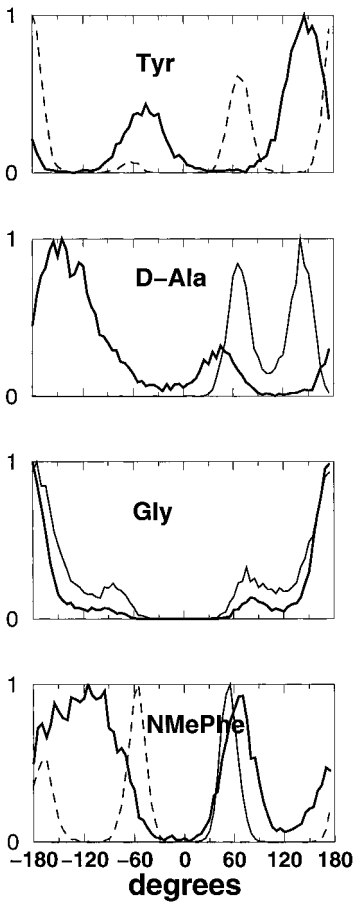

FIGURE 6 Distribution of dihedral angles during a 6.3-ns simulation of solvated DAMGO. Angles shown: ϕ (*thin line*), ψ (*heavy line*), χ_1 (*dashed line*).

DISCUSSION

The NMR data of *trans*-[D-Pro^2]EM1 in DMSO-d_6 outline a well-defined conformation with stacking of the Tyr, Pro, and Trp rings. These results are in sharp contrast with previous NMR data of *trans*-EM1 in DMSO-d_6, where only few NOE could be discerned, while *cis*-EM1 adopted a more compact conformation (Podlogar et al., 1998). The relevance of the NMR-derived structures to the loss of biological activity upon inversion of chirality at Pro is better understood by comparing the *trans*-EM1 (Podlogar et al., 1998) and *trans*-[D-Pro^2]EM1 structures. *Trans*-EM1 and *trans*-[D-Pro^2]EM1 were overlapped using the same conformation of the tyramine moiety, with ψ(Tyr) = 140° and χ_1(Tyr) = *t*, as shown in Fig. 7. Results on Tyr-Pro peptide fragments indeed suggest that the chirality of the proline residue does not change the conformational preference of the preceding tyrosine (Table 3). However, the residues following proline are directed to different spatial regions, because of inversion of the ϕ(Pro) dihedral angle. Stereochemical inversion at Pro results in an opposite spatial arrangement of Trp in the two peptides (Fig. 7), as the NMR data showed NOE cross-peaks between Trp and Pro side chains in the inactive diastereoisomer, while these were absent in EM1 (Table 2 and Podlogar et al., 1998). The fourth position, Phe^4, while less structurally defined, occupies distinct spatial regions in the two peptides.

Molecular dynamics (MD) simulations in explicit solvent provided additional insight into the structural properties of the peptides. In agreement with the NMR results, MD trajectories showed stacking of Tyr, Pro, and Trp side chains (structure A in Fig. 5 *a*) in [D-Pro^2]EM1 but not in EM1 (Podlogar et al., 1998). Simulations mirrored the relative rigidity of the Tyr-Pro-Trp region, as only two conformers were populated in both peptides (conformations A and B in Fig. 5 *a* and Podlogar et al., 1998). The lack of structural cross-peaks in the NOESY spectrum in water may then be explained in terms of equilibrium between these two conformations, while only one (A) is populated in DMSO. The Phe residue, on the other hand, was free to sample the conformational space, in agreement with the NMR data, in which the NOE correlation of the Phe aromatic ring with other side chains was not observed.

The ability of [D-Tyr^1] and [D-Trp^3] to fully activate the μ-receptor, albeit with greatly reduced potency, may originate from partial similarity with the putative bioactive conformation of EM1. MD trajectories of the backbone atoms in the Pro-Trp-Phe of [D-Tyr^1]EM1 are indeed similar to those obtained for EM1 (Podlogar et al., 1998), indicating that D-Tyr^1 samples its conformational space independently of the other residues. Using those conformations with ψ(Tyr) = 65° and χ_1(Tyr) = g^- (Fig. 5 *b*), it is possible to overlap [D-Tyr^1]EM1 with EM1, while the orientation of the nitrogen group differs by ~60° compared to EM1 (Fig. 7 and Table 4). The precise orientation of the Trp side chain

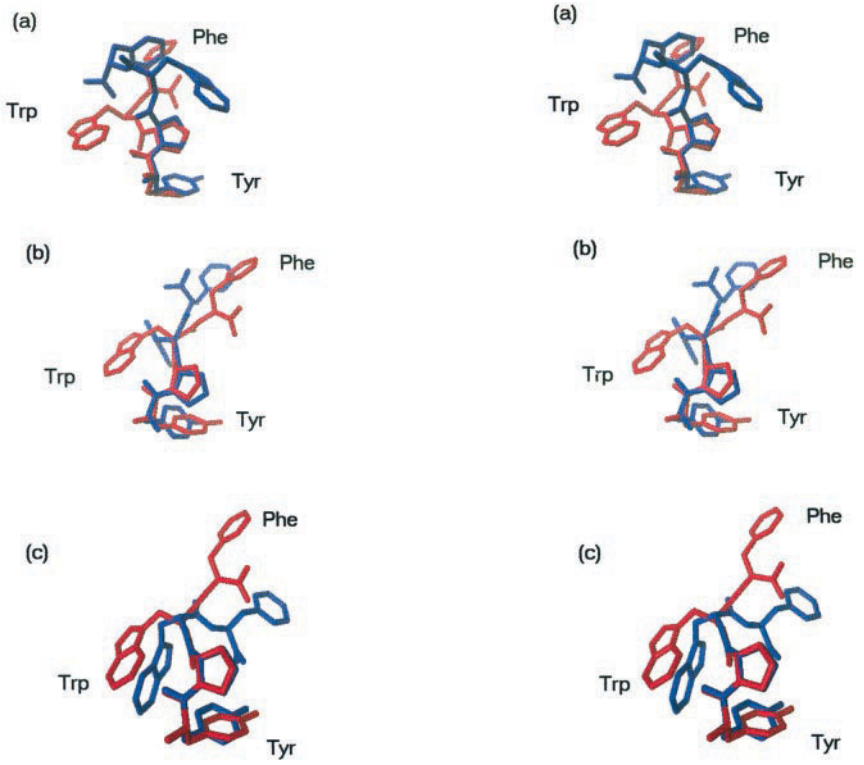

FIGURE 7 Comparison of EM1 (shown in *red*) with [D-Pro^2]EM1 (*a*), [D-Tyr^1]EM1 (*b*), and [D-Trp^3]EM1 (*c*) (shown in *blue*). Representative NMR-derived structures are chosen for the [D-Pro^2]EM1 and EM1 peptides. Conformation A of Fig. 5 is used for [D-Tyr^1]EM1.

is left undetermined by the overlap, as only the *t* rotamer was observed in MD trajectories of [D-Tyr^1]EM1, while g^+ and g^- conformations where observed as well for EM1 (Podlogar et al., 1998). The more severe reduction in potency upon chirality inversion at Trp suggests that this residue is more critical for receptor recognition.

A conformational search was conducted for [D-Trp^3]EM1 by systematically varying the ψ(Pro), ϕ(Trp), ψ(Trp), and χ_1(Trp) angles of [D-Trp^3]EM1 for a total of 648 starting conformations. Of these, 49 unique structures were found within 5 kcal/mol of the energy minimum. Conformations with backbone dihedral angles similar to those of EM1 were found within this set, but stereochemical inversion did not allow precise geometrical overlap of the Trp side chains (Fig. 7 and Table 4). The lower potency of the [D-Tyr^1]EM1 and [D-Trp^3]EM1 peptides may therefore be attributed to the fact that conformations with arrangement of the backbone dihedral angles similar to those of EM1 became energetically less favored (i.e., less populated) upon stereochemical inversion. Alternatively, the peptides may assume a less than ideal geometry of the three groups responsible for key interaction with the μ-receptor, i.e., the charged ammonium group and the Tyr and the Trp side chains. The effect of stereochemical substitution becomes less detrimental farther away from Pro (Table 1). The phenylalanine residue samples its conformational space independently of the other residues, as shown by the NMR data and MD simulations of EM1 (Podlogar et al., 1998), [D-Pro^2]EM1 (Table 5), and [D-Tyr^1]EM1 (Fig. 5), and a similar behavior is therefore expected for [D-Phe^4]EM1. These results suggest that Phe^4 is free to adopt a "bioactive" conformation at the receptor site and that activation can occur independently of the correct orientation and stereochemistry of this residue.

The solution structure of DAMGO has previously been determined using NMR spectroscopy and conformational analysis simulations (Penkler et al., 1993). A folded con-

TABLE 4 Torsion angles of the NMR and simulated structures of endomorphin-1 and diastereoisomers used in the structural comparison*

	Tyr		Pro		Trp			Phe		
Peptide	ψ	χ_1	ϕ	ψ	ϕ	ψ	χ_1	ϕ	ψ	χ_1
t-EM1†	133	−174	−61	166	−113	−32	−85	−124	120	−178
t-[D]-Pro^2]EM1‡	136	−174	68	139	−72	−34	−35	−127	157	45
t-D-Tyr^1]EM1	65	−73	−74	146	−140	165	−167	−74	151	−167
t-[D-Trp^3]EM1	136	−175	−59	163	−61	17	−78	−149	−56	−171

*Angles are in degrees.
†From Podlogar et al. (1998).
‡NMR-derived structure.

TABLE 5 ^{1}H and ^{13}C chemical shifts of [D-Pro^{2}]EM1 in DMSO-d_6 at 25°C

Peak	*cis*	*trans*
Y_{NH}	8.11 (broad)	
Y_{α}	4.24	
Y_{β}	2.92/2.87	
Y_{OH}	9.41	9.29
$Y_{2,6}$	7.01 (123.42)	
$Y_{3,5}$	6.70 (114.32)	6.66
P_{α}	4.22	4.67, 4.30
P_{β}	1.62/1.35 (27.94)	1.88/1.45, 1.80/1.48
$P\gamma$	1.58/1.38 (23.02)	1.64
P_{δ}	3.44 (49.73)	3.51
P'_{δ}	2.74	2.82
W_{NH}	8.18	8.30
W_{α}	4.42	4.78, 4.51, 4.38
W_{β}	3.11/2.80	3.17/2.96, 2.92/2.77
W_1	10.75	10.80
W_2	7.05 (126.84)	7.07
W_4	7.52 (119.86)	7.59
W_5	6.47	
W_6	6.96	7.07
W_7	7.30	7.29
$W_{\varepsilon 2}$	(135.04)	
$W_{\delta 2}$	(126.25)	
F_{NH}	7.95	7.79
F_{α}	4.49	4.47
F_{β}	3.03/2.84	3.04/2.88
$F_{2,6}$	7.33	
$F_{3,5}$	7.39	

^{13}C chemical shifts are in parentheses. All values are ppm.

formation, characterized by a β-II-like turn around Gly^{3}-MePhe^{4}, was proposed for the *trans* isomer of this peptide, but NMR experiments were not able to fully resolve the structure of this peptide. Structural uncertainty in the "hinge region" resulted in structures with a wide range of distances and orientations between the two aromatic residues. Molecular dynamics simulations of *t*TAGP obtained in this work mirrored the flexibility of this peptide in solution. However, comparison with the more rigid EM1 also revealed structural similarities between these two peptides. An overlap between EM1 and representative DAMGO conformers taken from the MD trajectory is shown in Fig. 8. The more favored χ_1(Tyr) = *t* rotamer (Penkler et al., 1993) was chosen in the overlap. The comparison shows that Tyr^{1}-MePhe^{4} of DAMGO and Tyr^{1}-Phe^{4} of EM1 can assume a similar orientation with a separation between the aromatic rings of ~12 Å. The Trp residue of EM1 clearly appears as an additional site, as overlap of this amino acid with MePhe^{4} does not occur. Recent studies comparing EM1 and DAMGO efficacy and potency at μ-opioid receptors have yielded different results, depending on the type of experiment performed and system used. EM1 has been reported to act as a partial agonist, based on [^{35}S]GTPγS binding (Alt et al., 1998; Harrison et al., 1998; Narita et al., 1998) and autoradiography assay (Sim et al., 1998), but it has been described as a full agonist in its ability to inhibit cAMP and activate inwardly rectifying K^{+} channels (Gong et al., 1998). The results shown here imply that the two peptides may bind and activate the μ-receptor in a similar fashion. However, the greater conformational flexibility of DAMGO compared to EM1 does not exclude the existence of additional binding modes for DAMGO.

CONCLUSIONS

NMR and simulations data have shown that Pro^{2} provides the necessary stereochemical requirements for activity of EM1 at the μ-opioid receptor. Proline directs Trp^{3} toward a μ-selectivity region in EM1, where the active conformation is characterized by a structure in which the Tyr^{1} and Trp^{3} side chains have opposite orientations with respect to Pro^{2}. Such orientation is reversed in [D-Pro^{2}]EM1, where side chain–side chain interactions occur between Trp^{3} and Pro^{2}. This change in orientation results in the inability to activate the receptor. The fourth residue of EM1 has a less stringent stereochemical or conformational requirement, as loss in potency is only 10-fold. Molecular dynamics simulations and NMR data indeed show that this position is conformationally flexible and independent of the preceding three

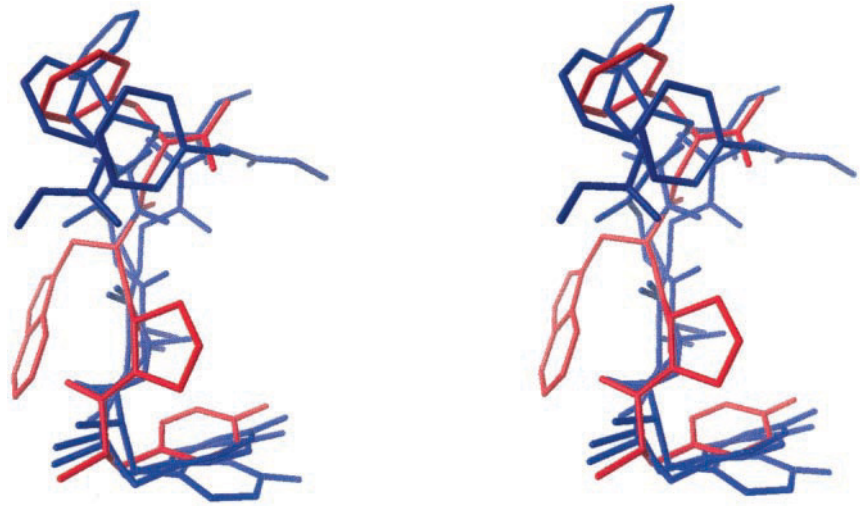

FIGURE 8 Overlap of EM1 (shown in *red*) with *t*TAGP (Tyr-D-Ala-Gly-MePhe-N′-CH_3) (shown in *blue*). Representative tTAGP conformers from the MD trajectory are aligned using a rms fit of the first three residue backbone atoms. EM1 is aligned with a rms fit of the nitrogen of Tyr and the Tyr^{1} and Phe^{4} side chains.

amino acids. The result that [D-Tyr^1]EM1, [D-Trp^3]EM1, and [D-Phe^4]EM1 have full intrinsic activity with reduced potency suggests that the region of the receptor responsible for interaction with Tyr^1 and Trp^3 can tolerate different orientations of these side chains and the tyramine chromophore. Whether there is more than one bound conformation or a single conformation that is responsible for receptor activation is not known. Comparison of EM1 and DAMGO indicates that the two peptides can adopt similar conformations, characterized by a Tyr^1-Phe^4/MePhe^4 distance of ~12 Å. However, EM1 has an additional recognition site at Trp, while the greater flexibility of DAMGO may allow additional binding modes. The implication of dynamical properties of opioid peptides in the activation of the μ-opioid receptors can be further explored by probing the binding of accessible conformers to opioid receptor models.

We thank Michael Powers for in vitro testing of the compounds.

This work was supported in part by Public Health Service grants DA-00377 (to MGP) and DA-01533 (to PSP). NMR instrumentation was provided with funds from the National Science Foundation (BIR-961477) and the University of Minnesota Medical School.

REFERENCES

Alt, A., A. Mansour, H. Akil, F. Medzihradsky, J. R. Traynor, and J. H. Woods. 1998. Stimulation of guanosine-5′-*O*-(3-[^{35}S]thio)triphosphate binding by endogenous opioids acting at a cloned *mu* receptor. *J. Pharmacol. Exp. Ther.* 286:282–288.

Amodeo, P., F. Naider, D. Picone, T. Tancredi, and P. A. Temussi. 1998. Conformational sampling of bioactive conformers: a low-temperature NMR study of ^{15}N-Leu-enkephalin. *J. Pept. Sci.* 4:253–265.

Carpenter, K. A., P. Schiller, R. Schmidt, and B. C. Wilkes. 1996. Distinct conformational preferences of the three cyclic β-casomorphin-5 analogs determined using NMR spectroscopy and theoretical analysis. *Int. J. Pept. Protein Res.* 48:102–111.

Case, D. A., D. A. Pearlman, J. W. Caldwell, T. E. Cheatham, W. S. Ross, C. L. Simmerling, T. A. Darden, K. M. Merz, R. V. Stanton, A. L. Cheng, J. J. Vincent, M. Crowley, D. M. Ferguson, R. J. Radmer, G. L. Seibel, U. C. Singh, P. K. Weiner, and P. A. Kollman. 1997. AMBER 5. University of California, San Francisco, CA.

Casy, A. F. 1993. The Steric Factor in Medicinal Chemistry: Dissymmetric Probes of Pharmacological Receptors. Plenum Press, New York.

Chang, K. J., A. Killian, E. Hazum, and P. Cuatrecasas. 1981. Morphiceptin (NH_4-Tyr-Pro-Phe-Pro-$CONH_2$): a potent and specific agonist for morphine (m) receptors. *Science.* 212:75–77.

Chang, K.-J., E. T. Wei, A. Killian, and J.-K. Chang. 1983. Potent morphiceptin analogs: structure activity relationships and morphine-like activities. *J. Pharmacol. Exp. Ther.* 227:403–408.

Cornell, W. D., P. Cieplak, C. I. Bayly, I. R. Gould, K. M. Merz, Jr., D. M. Ferguson, D. C. Spellmeyer, T. Fox, J. W. Caldwell, and P. A. Kollman. 1995. A second generation force field for the simulation of proteins, nucleic acids and organic molecules. *J. Am. Chem. Soc.* 117:5179–5197.

Delagio, F., S. Grzesiek, G. W. Vuister, G. Zhu, J. Pfeifer, and A. Bax. 1995. NMRPipe: a multidimensional spectral processing system based on UNIX pipes. *J. Biomol. NMR..* 6:277–293.

Dorman, D. E., and F. A. Bovey. 1973. Carbon-13 magnetic resonance spectroscopy. The spectrum of proline in oligopeptides. *J. Org. Chem.* 38:2379–2383.

D'Ursi, A., M. Pegna, P. Amodeo, H. Molinari, A. Verdini, L. Zetta, and P. A. Temussi. 1992. Solution conformation of tuftsin. *Biochemistry.* 31:9581–9586.

Gong, J., J. A. Strong, S. Zhang, X. Yur, R. N. Dehaven, J. D. Dauber, J. A. Cassel, G. Yu, E. Mansson, and L. Yu. 1998. Endomorphin fully activates a cloned human mu opioid receptor. *FEBS Lett.* 439:152–156.

Harrison, L. M., A. J. Kastin, and J. E. Zadina. 1998. Differential effects of endomorphin-1, endomorphin-2, and Tyr-W-MIF-1 on activation of G-proteins in SH-SY5Y human neuroblastoma membranes. *Peptides.* 19:749–753.

Higashijma, T., J. Kobayashi, U. Nagai, and T. Miyazawa. 1978. Nuclear magnetic resonance study on Met-enkephalin and Met-enkephalinamide. *Eur. J. Biochem.* 97:43–57.

Kimura, A., N. Kuni, and H. Fujiwara. 1997. Conformation and orientation of Met-enkephalin analogues in a lyotropic liquid crystal studied by the magic-angle and near-magic-angle spinning two dimensional methodology in nuclear magnetic resonance: relationships between activities and membrane-associated structures. *J. Am. Chem. Soc.* 119:4719–4725.

Milon, A., T. Miyazawa, and T. Higashijima. 1990. Transferred nuclear Overhauser effect analyses of membrane-bound enkephalin analogues by ^{1}H nuclear magnetic resonance: correlation between activities and membrane-bound conformations. *Biochemistry.* 29:65–75.

Mosberg, H. I., R. Hurst, V. J. Hruby, K. Gee, H. I. Yamamura, J. J. Galligan, and T. F. Burks. 1983. Bis-penicillamine enkephalins possess highly improved specificity toward delta opioid receptors. *Proc. Natl. Acad. Sci. USA.* 86:5188–5192.

Narita, M., H. Mizoguchi, G. S. Oji, E. L. Tseng, C. Suganuma, H. Nagase, and L. F. Tseng. 1998. Characterization of endomorphin-1 and -2 on [^{35}S]GTPγS binding in the mouse spinal cord. *Eur. J. Pharmacol.* 351:383–387.

Némethy, G., K. D. Gibson, K. A. Palmer, C. N. Yoon, M. G. Paterlini, A. Zagari, S. Rumsey, and H. A. Scheraga. 1992. Energy parameters in polypeptides. 10. Improved geometrical parameters and nonbonded interactions for use in the ECEPP/3 algorithm, with application to proline-containing peptides. *J. Phys. Chem.* 96:6472–6484.

Penkler, L. J., P. H. van Rooyen, and P. L. Wessels. 1993. Conformational analysis of μ-selective [D-Ala^2,MePhe^4]enkephalins. *Int. J. Pept. Protein Res.* 41:261–274.

Picone, A., A. D'Ursi, A. Motta, T. Tancredi, and P. A. Temussi. 1990. Conformational preferences of [Leu^5]enkephalin in biomimetic media: investigation by ^{1}H NMR. *Eur. J. Biochem.* 192:433–439.

Podlogar, B. L., M. G. Paterlini, D. M. Ferguson, G. C. Leo, D. A. Demeter, F. K. Brown, and A. B. Reitz. 1998. Conformational analysis of the endogenous μ-opioid agonist endomorphin-1 using NMR spectroscopy and molecular modeling. *FEBS Lett.* 439:13–20.

Portoghese, P. S., A. W. Lipkowski, and A. E. Takemori. 1987. Binaltorphimine and nor-binaltorphimine, potent and selective κ-opioid receptor antagonists. *Life Sci.* 40:1287–1292.

Portoghese, P. S., and A. E. Takemori. 1985. TENA, a selective kappa opioid receptor antagonist. *Life Sci.* 36:801–805.

Rang, H. P. 1964. Stimulant actions of volatile anaesthetics on smooth muscle. *Br. J. Pharmacol.* 22:356–365.

Schiller, P. W., T. M.-D. Nguyen, G. Weltrowska, B. C. Wilkes, B. J. Mardsen, C. Lemieux, and N. N. Chung. 1992. Differential stereochemical requirements of μ vs. δ opioid receptors for ligand binding and signal transduction: development of a class of potent and highly δ-selective peptide antagonists. *Proc. Natl. Acad. Sci. USA.* 89:11871–11875.

Schwartz, R. W., A.-C. Chang, P. S. Portoghese, and I. B. Berzetei-Gunske. 1997. A guinea pig ileum preparation devoid of functional κ-receptors: a new in vitro pharmacologic assay for functional μ opioid ligands. *Life Sci*. 60:PL235–PL239.

Sim, L. J., Q. Liu, S. R. Childers, and D. E. Selley. 1998. Endomorphin-stimulated [^{35}S]GTPγS binding in rat brain: evidence for partial agonist activity at μ-opioid receptors. *J. Neurochem*. 70:1567–1576.

Stahl, M. T., and W. P. Walter. 1995. PADRE, Population Analysis, and Duplicate Removal. Harvard University Chemistry Labs, Cambridge, MA.

Williamson, M. P., T. F. Havel, and K. Wüthrich. 1985. Solution conformation of proteinase inhibitor IIA from bull seminal plasma by ^{1}H nuclear magnetic resonance and distance geometry. *J. Mol. Biol.* 182:295–315.

Zadina, J. E., L. Hackler, L.-J. Ge, and A. J. Kastin. 1997. A potent and selective endogenous agonist for the μ-opiate receptor. *Nature.* 386: 499–502.